Available online at www.sciencedirect.com

SciVerse ScienceDirect

Ceramics International 39 (2013) 5327–5333

CERAMICS INTERNATIONAL

www.elsevier.com/locate/ceramint

Characterization of textured ceramics containing mullite from phyllosilicates

K. Boussois[a], S. Deniel[a], N. Tessier-Doyen[a], D. Chateigner[b], C. Dublanche-Tixier[c], P. Blanchart[a,c,*]

[a]GEMH, ENSCI, 12 rue Atlantis, 87068 Limoges, France
[b]CRISMAT-ENSICAEN, Université de Caen Basse Normandie 14050, Caen, France
[c]SPCTS, ENSIL, Université de Limoges, 87068 Limoges, France

Received 18 September 2012; received in revised form 11 December 2012; accepted 12 December 2012
Available online 1 January 2013

Abstract

Organized ceramics are obtained from kaolinite and muscovite suspensions and shaped by aqueous tape casting or centrifugation. These processes favor the preferential orientation of particles in the powder compact. After sintering at 1400 °C, this study analyzed sample microstructures using QTA to determine the degree of the mullite orientation. The analyses revealed two main texture components, a planar texture along the *c*-axis of the mullite and a preferred orientation along the *a*-axis, which were aligned parallel and perpendicular to the casting plane, respectively. The important role of processing parameters in the organization degree of the mullite was apparent during the study. The elastic properties at different measurement scales were obtained using US echography and nanoindentation and were closely related to the organization degree of the mullite crystals obtained from the QTA analyses that were consistent with the development of an interconnected mullite network. The Young's moduli due to the nanoindentations were also determined parallel and perpendicular to the layers, and indicated the samples' anisotropic behavior. Both the Young's modulus and the anisotropy of the Young's modulus were correlated with the texture index. In particular, the anisotropy of the Young's moduli was linearly related to the overall texture index, highlighting the microstructures' anisotropic nature.

Keywords: A. Tape casting; C. Mechanical properties; D. Mullite; Pole figures (QTA)

1. Introduction

Ceramic materials with organized microstructures can be obtained from powder compacts with anisotropic grains using specific shaping processes for tape casting and centrifugation.

Tape casting [1,2] consists of spreading a suspension on a fixed support composed of a flat piece of glass coated with a Mylar film and is also called Doctor Blading. This forming method has the advantage of producing laminated green tapes with uniform thickness, density and surface flatness. Tape-casting is used extensively for the manufacture of substrates and multilayer structures, and uses a mixture of powders, solvents and various additives as dispersants and plasticizers. Non-aqueous organic solvents are commonly used because they improve the rheology of highly concentrated slurries and accelerate the drying process of green tapes. However, slurry formulations that contain water have also been successfully used with different powder types [3,4]. The slurry formulation requires water-soluble binders, plasticizers and dispersants in amounts that are highly dependent on powder type, granulometry and relative concentration. Because lamination always occurs during tape casting, it induces the preferential orientation of elongated and sheet particles, as phyllosilicates, in the direction plane to the tape direction.

Centrifugation can also be used to obtain oriented powder compacts from aqueous suspensions of various anisotropic grains as phyllosilicates [5]. During the centrifugation process,

*Corresponding author at: GEMH, ENSCI, 12 rue Atlantis, 87068 Limoges, France. Tel.: +33 87 502 300.
E-mail address: philippe.blanchart@unilim.fr (P. Blanchart).

0272-8842/$ - see front matter © 2012 Elsevier Ltd and Techna Group S.r.l. All rights reserved.
http://dx.doi.org/10.1016/j.ceramint.2012.12.038

the compaction at the powder's equilibrium results from the accelerated settling of suspensions along the z-axis of a container, which forms thick layers measuring up to 4 mm.

During the sintering of green powder compacts, oriented grains induce specific recrystallization processes [6], leading to ceramics with improved properties, including mechanical properties, because the morphology, orientation degree and connectivity of the crystals in the microstructures determine these macroscopic properties.

Mullite crystallization always forms elongated shapes in silicate ceramics obtained from clay minerals. The extent to which this phenomenon occurs depends on the clay mineral type, morphology and relative quantity in the initial composition. In previous studies, we have reported that the kaolinite-muscovite interaction during sintering favors the crystallization and growth of needle-like mullite crystals, oriented in the initial musocvite's preferential crystallographic directions [7,8]. The 3D interlocking mullite network within the glassy matrix has favored the increase of mechanical properties [9], and the material's mechanical behavior has also been found to depend on the pore shapes and distributions in the microstructures [10,11]. These properties can be changed by controlling the starting composition and grain size of the materials, as well as by the optimization of the different processing parameters involved in the shaping methods [12].

The objective of this study was to obtain silicate ceramics with an organized microstructure, containing mullite, to improve their mechanical properties. The materials were shaped by the aqueous tape casting of concentrated suspensions composed of kaolin and muscovite powders. Centrifugation of the aqueous suspensions was also used to compare the results between the two methods. The shaping and sintering processes were optimized to favor the formation of a 3D network of mullite within the microstructures. The mechanical properties at the microscopic and macroscopic scales were characterized and correlated with the microstructural characteristics, mullite orientation degree and porosity of the material.

2. Experimental procedure

The tape cast slurries were prepared using three steps. First, aqueous suspensions were prepared by grinding kaolin (BiP, Denain-Anzin-Minéraux) in a planetary mill (Fritsch, Pulverisette; 80 min; 180 rpm) with an anti-foaming agent (Constraspum; 0.1 wt%) and a dispersant (Dolaflux, 0.3 wt%). Next, a binder (PVA 22000; 5 wt%) and a plasticizer (PEG 300, 5 wt%) were added to the suspension and mixed for 6 h at a low speed (100 rpm). Finally, muscovite mica (Micromica 3251, 10 wt%) was ball milled with the suspension for 1 h at 100 rpm in quantities of 0% and 5% wt.

The tape casting was performed with non-continuous laboratory equipment ($500 \times 50\ mm^2$) with which the spreading rate and thickness of the green tapes (500 μm) could be precisely monitored. The green tapes were dried at room temperature for 12 h, after which cylindrical samples ($\phi = 30$ mm) were cut from the green tapes and stacked in eight individual layers at a controlled temperature and pressure ($T = 60\ ^\circ C$; $p = 50$ bars). After a debinding stage, (800 °C, 1.5 °C min^{-1}), sintering was performed at a heating rate of 5 °C/min and at a maximum temperature of 1410 °C over 2 h. The density and porosity of the sintered samples were measured using Archimedes's method and helium pycnometry, respectively.

Centrifugation (Sigma 301) was performed on an aqueous suspension of the same kaolin. The range of processing parameters and compositions used has been previously described in Ref. [5]. The suspensions were prepared by grinding kaolin particles in water with a dispersant (Dolaflux, 0.2 wt%) in a planetary mill (Fritsch, Pulverisette, 40 min, 180 rpm). The suspensions were placed in cylindrical containers perpendicular to the rotation axis of the centrifuge. The experiments lasted 10–30 min to obtain the samples' relative density equilibrium, defined by a constant thickness of the powder compact and resulting in disc-shaped samples (diameter of 36 mm and height 1–5 mm).

The determination of the sintered ceramics' elastic properties was carried out using nanoindentation (NanoXP^{TM}, MTS Instruments) with a Berkovich tip in a continuous stiffness measurement mode (CSM) [13,14]. The penetration depth was set at 2000 nm so that the indented area would account for the influence of heterogeneities at the grain scale. The anisotropy of the samples was obtained from measurements (with a mean of 40 indents) carried out in directions parallel and perpendicular to the tape casting directions (r and z, respectively).

Characterizations at the macroscopic scale were investigated using ultrasonic echography operated in immersion (frequency of 80 MHz) to determine the Young's moduli in the r and z directions.

The fracture strengths were obtained with biaxial disc flexure in a piston-on-ring assembly with previously polished samples. The results for 10 samples were used to compute the mean and standard deviation.

To quantify the crystal orientation, a quantitative texture analysis (QTA) was performed using a four-circle diffractometer, allowing for the acquisition of the entire diffraction pattern, up to 80° 2θ, for each tilt angle χ and azimuth angle φ of the sample's orientation. Diagrams were acquired for many sample orientations using a $5^\circ \times 5^\circ$ measuring grid in (χ,φ), up to $\chi = 55^\circ$. The entire data set was analyzed using Whole-Powder-Pattern Rietveld analysis within the combined analysis formalism [15] and the orientation distribution functions were refined using the E-WIMV approach [16]. The pole figures were plotted using an equal area projection on the disc plane, with their center set in the r direction. The intensities were normalized into distribution densities using multiples of a random distribution (MRD) units. The overall texture strength was evaluated using the texture index [15] and the normalization of the pole figures into MRD values was performed during the orientation distribution (ODF) refinement of the crystallites during the

E-WIMV step. The ODF and profile refinement reliabilities were estimated using conventional reliability factors [17].

3. Results

Table 1 presents the range of processing parameters used for shaping the samples that had a significant influence on the samples' microstructural characteristics.

The porosity of the materials after sintering at 1410 °C for 2 h is shown in Table 2, in which the muscovite content varies from 0 to 5 wt%. The table indicates that the addition of 5 wt% of muscovite favored the increase of both open and closed porosity.

The Rietveld analyses of the XRD patterns first revealed that the only crystalline phase was 3:2 mullite, and it coexisted with an amorphous phase. Considering that the amorphous phase was similar to an alkaline silico-aluminate, Rietveld fits were obtained with good reliability factors, and a typical example of this fit is shown in Table 3 for a kaolinite/muscovite material (sample TC7 in Table 1). The refined cell parameters were $a=7.553$ Å, $b=7.686$ Å, and $c=2.886$ Å, which are similar to the data in literature [18,19]. Quantitative Texture Analysis of the same sample's XRD patterns gave the pole figures in Fig. 1 for {001}, {020} and {200} mullite orientations, the first direction being in plane with the tape surface. The overall texture index and fraction of texture components were determined from the inverse pole figures in Fig. 2, which are plotted for the main sample directions r (ND), x (RD) and y (TD). The overall texture index of this material was 1.77MRD^2, and this value can be compared in Table 1 with the texture indices of different samples obtained either by tape casting or centrifugation. The main processing parameters are also reported in Table 1 to show how the processing parameters change the texture index.

Using sample TC7 obtained by tape casting, from Table 1, obtained Table 4 presents the Young's modulus measured in the directions parallel (E_r) and perpendicular (E_z) to the casting plane, when the muscovite quantity changes. Using US echography, the addition of muscovite induced a slight variation in both E_r and E_z, but decreased the anisotropy of the elastic properties (E_r-E_z). When indentation was used at a more local scale, the E_r and E_z values significantly decreased, but the anisotropy of the elastic properties increased. The variations in E_r and E_z were very similar for samples obtained from the centrifugation process.

The Texture Index in Table 1 was correlated with the Young's Modulus in the r and z directions from samples obtained by both centrifugation and tape casting (Fig. 3).

Table 3
Reliability factors and cell parameters for the Rietveld and ODF analyses of a kaolinite+muscovite material (sample TC7 in Table 1).

Analysis method		Reliability factors
Rietveld analysis	R_w	15.9
	R_B	12.6
Orientation distribution refinement (ODF)	R_w	8.2
	R_B	8.7
Cell parameters (Å)	a	7.553
	b	7.686
	c	2.886

Table 1
Processing parameters used for shaping the samples by centrifugation or tape casting. The C series was obtained from centrifugation (previous study [5]) and the TC sample was obtained from tape casting. The texture indices obtained with QTA are also reported.

Sample	Kaolin (vol%)	Mica (vol%)	Centrifugation height (mm)	Dispersant (wt%)	PVA (wt%)	PEG (wt%)	Stacking mode	Heating rate (°C/min)	Overall texture index (MRD^2)
C 1	25	–	9.8	–	–	–	–	5	1.14
C 2	25	–	11.2	–	–	–	–	15	1.17
C 3	25	–	11.2	–	–	–	–	5	1.22
C 4	22.5	2.5	11.2	–	–	–	–	5	1.77
C 5	22.5	2.5	11.2	–	–	–	–	15	1.68
C 6	20	5	11.2	–	–	–	–	5	1.34
TC 7	38	3.8	–	0.27	5	5	90°	5	1.77

Table 2
Porosity of the tape cast materials with muscovite content varying from 0 to 5 wt%.

Composition	Total porosity (%)		Open porosity (%)		Closed porosity (%)	
	Average	S.D.	Average	S.D.	Average	S.D.
Kaolinite	6.4	0.6	0.5	0.2	5.7	0.7
Kaolinite–mica	15.2	0.9	4.1	2.3	12.4	1.8

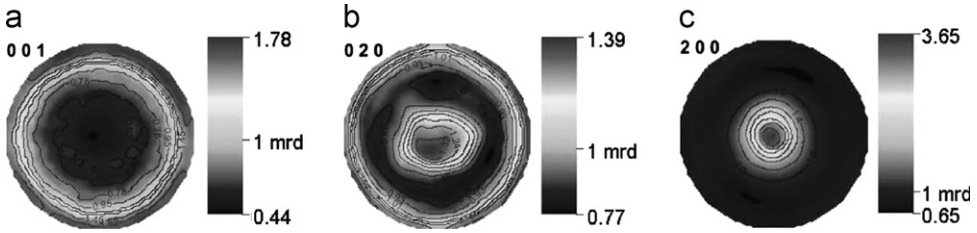

Fig. 1. Pole figures of the mullite axes in a kaolinite–muscovite material (sample TC7 from Table 1). (a): {001}; (b): {200}; and (c): {020}.

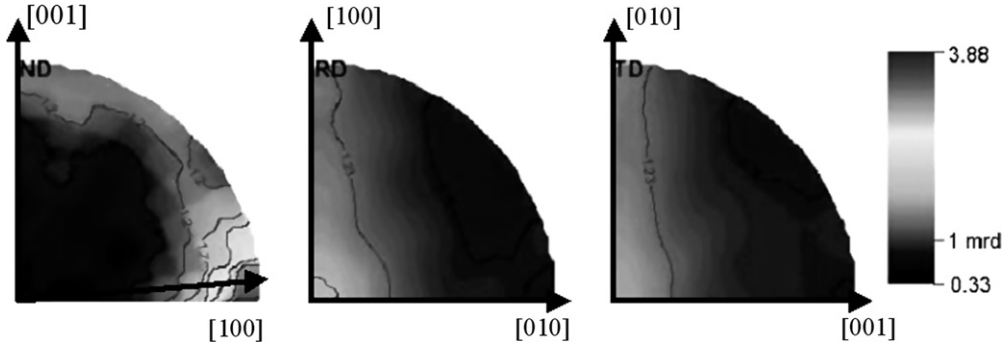

Fig. 2. Inverse pole figures for the main sample directions in sample TC7 from Table 1: r (ND), x (RD) and y (TD).

Table 4
Results for sample TC7 created using tape casting, including the influence of a muscovite addition (5 wt%) on the Young's modulus along the r-axis (E_r) and z-axis (E_z). The measurement techniques were indentation at a 2000-nm depth and US echography.

Composition type			Kaolinite	Kaolinite–mica
Indentation at 2000 nm	E_r (GPa)	Average	114	98
		S.D.	4	5
	E_z (GPa)	Average	117	109
		S.D.	6	6
US echography	E_r (GPa)	Average	98.4	100.0
		S.D.	4.9	8
	E_z (GPa)	Average	93.3	91.1
		S.D.	0.3	2.6

In samples obtained from centrifugation, the general trend was a slight increase in the elastic properties with the increase in texture index to a value of 1.4MRD^2. A plateau was observed above this value. A similar trend was assumed with the tape casted samples, but the lack of supplementary data necessitated future experimentation.

In a similar way, the flexural strength of the samples obtained by both centrifugation and tape casting are presented in Fig. 4 as a function of the texture index. The strength follows the same trend as the elastic properties for the centrifuged samples. One result from the tape casting process shows a much higher value, and therefore an increasing trend with increasing texture index can be assumed.

4. Discussion

Fig. 1 shows that the addition of muscovite favors an increase in porosity, which varies approximately from 6.6 to 15.5 vol%, regardless of layer thickness. This result was due mainly to closed porosity induced by the exfoliation of muscovite in the 600–900 °C temperature range [20].

The quantitative texture analysis of a representative material (sample TC 7 in Table 1) for the {001}, {020} and {200} directions of mullite are given in the pole figures of Fig. 1. The {001} pole figure in Fig. 1 shows that the c-axis is aligned parallel to the sample plane, or the casting direction. The axis forms a planar texture when the maximum orientation density is located at the periphery of the {001} pole figures and reaches 1.77MRD. The orientation density is uniformly distributed at the periphery of the figure, indicating that the tape casting process leads to a quasi-uniformly oriented mullite in-plane of layers. The minimum value of the {001} pole figure indicates that only 44 vol% of the material is not oriented within the planar texture.

Because other crystallographic directions are supposed to be randomly distributed from the c-axis, a broad maximum

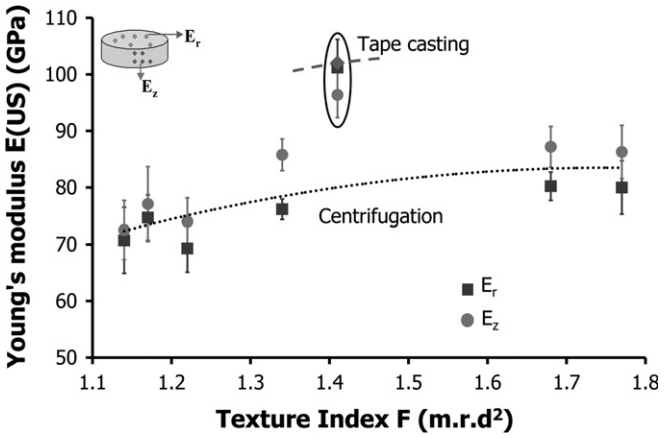

Fig. 3. Correlation of the Young's modulus obtained with US echography to the texture index obtained with QTA. Data are from samples obtained by either centrifugation or tape casting.

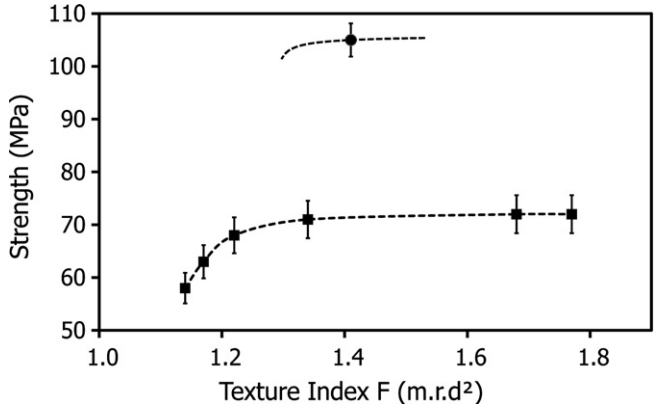

Fig. 4. Correlation of the flexural strength with the texture index obtained with QTA. Data are from samples obtained by either centrifugation or tape casting.

should be observed in the center of any {hk0} pole figure. Accordingly, the centers of the {020} and {200} figures (Fig. 1) have a maximum of 1.39MRD and 3.65MRD, respectively. However, in the {020} pole figure (Fig. 1), a supplementary orientation density is located at the periphery that indicates the coexistence of a planar component. This observation is consistent with the existence of a second texture component shown in Fig. 1, a $<200>$ preferential orientation. This component is predominant in the material with a 3.65MRD orientation density.

The orientations are also observed in the inverse pole figures calculated from the ODF function for the 3 directions (Fig. 2). A slight accentuation occurs in the RD and TD directions of the samples for the $<001>$ and $<010>$ orientations, which indicate a planar texture. A more accentuated texture index is also observed in the ND figure in the $<100>$ direction, which further indicates a $<100>$ fiber-like texture. This result confirmed that the mullite *a*-axis was parallel to the casting plane. The minimal value of the ODF indicated that 33 vol% of the material was not in the main orientation direction, and the maximum OD texture index was 3.88MRD^2, revealing a relatively high texture strength.

In Table 4, the characterization of the elastic properties shows that the addition of muscovite improves the orientation degree of the mullite. Whatever the shaping parameters being studied, the difference $(E_r - E_z)$ was dependent on the measurement technique because it increased significantly when indentation was used, but did not vary with the E_{US} measurements. An initial explanation of this phenomenon came from the measurement scale because indentation at a 2000-nm depth was a micro-scale characterization, while the ultrasonic echography gave information at the macroscopic scale (mm). Fig. 5a shows mullite crystals of approximately a

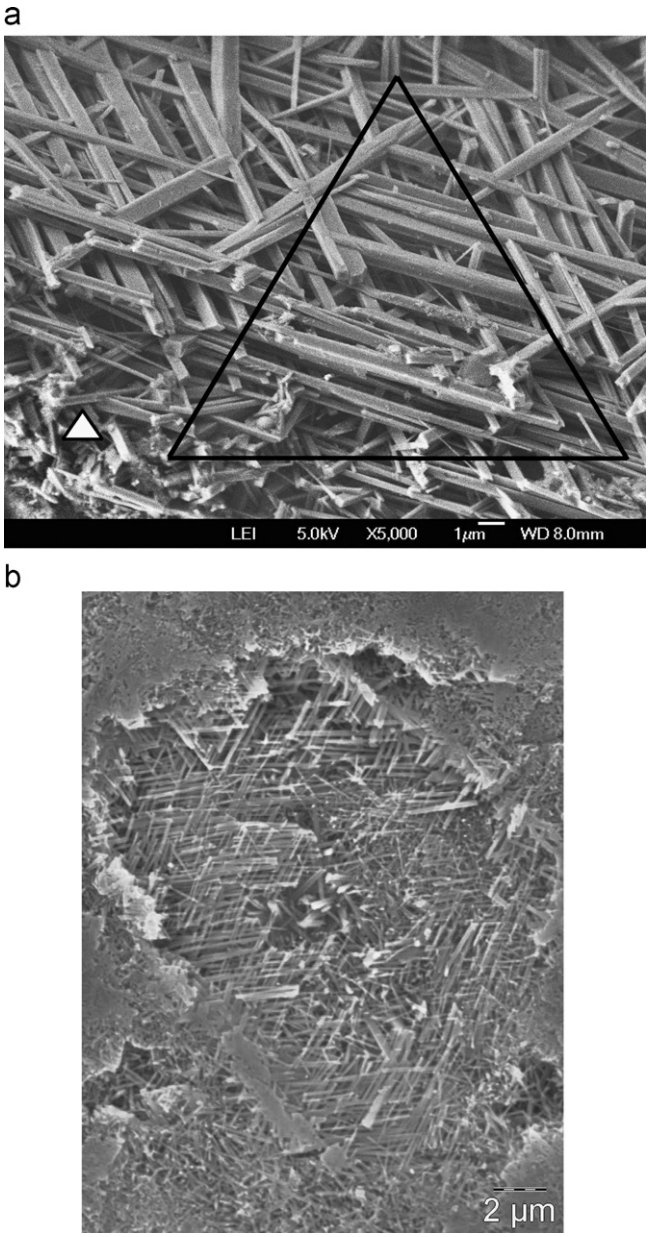

Fig. 5. Representation of: (a) indentation size at 100 nm and 2000 nm depths relative to mullite size on the surface of kaolinite+muscovite and (b) mullite distribution along the casting plane, showing local disorientations and flaws at the micrometric scale.

few microns along the *c*-axis and of 0.1–0.2 μm along the *a*- and *b*-axes. By comparison, the indent diagonals are approximately 6–8 μm when a 2000-nm depth is used. Such an indentation size allows for the measurement of the Young's modulus over a few tens of needles and is greater than the size of any local flaws, which are seen in Fig. 5b. The indentation averages local measurements but remains sensitive to mullite orientations at a low scale, which ensures the significance of the measurements.

At a lower scale, the Berkovich nanoindentation at a 100-nm depth, instead of micro-indentation, led to a 400-nm indentation size, also indicated in Fig. 5a. In that case, only 1–2 crystals were measured that greatly increased the distribution of the results, due to the heterogeneous state of the material at the nanoscale. The disorientation of the mullite crystals from that of the Berkovich tip was determinant because the elastic components of the mullite given by literature [21] differ along the measurement axes (Fig. 5a). Nanoindentation is preferentially related to the E_{11} (232 GPa) and E_{22} (167 GPa) components, which are the weakest compared to $E_{33}=282$ GPa. The elastic components in all 3 directions are considered with the ultrasonic echography technique.

The role of porosity in mechanical properties is also essential to the fracture strength and Young's modulus. The usual expression for the Young's modulus-porosity relationship [22] was used to calculate the intrinsic (i.e., without porosity) Young's modulus of the material, E_0. In Table 5, $E_0(r)$ and $E_0(z)$ in the *r* and *z* directions are calculated using E_{exp} in the two directions. On the other hand, the increase in porosity shows that the $E_0(r)$ and $E_0(z)$ values are significantly increased by the addition of muscovite. This result indicated that porosity was not the predominant parameter for the macroscopic properties of the materials.

The influence of the shaping process on the material properties was obtained from the tape casting and centrifugation results. In a previous study [5], the centrifugation technique has shown the influence of microstructural orientation on the properties, and in this study it was shown using the global texture index *F* from the QTA (Quantitative Texture Analysis).

Fig. 3 shows the correlation of the Young's modulus obtained using US echography with that obtained by the texture index using QTA. Considering that the data were obtained from centrifugation, a simple correlation between the Young's modules E_{US} along the *r* and *z*-axes and the texture index could be found regardless of the qualitative regression method used. The results showed that a first increase was followed by a plateau value above a texture index of 1.5MRD^2. Using the porosity data for all the samples, a similar variation was obtained with the E_0 values, meaning that the porosity led to an almost constant shift in Young's modulus values. A similar variation compared to the texture index should be assumed for a sample obtained by tape casting with a higher Young's modulus (Fig. 3). In that case, the optimal texture index must be determined with further experimentation.

The change in fracture strength is also dependent on the texture index and shaping process (Fig. 4). As for the elastic properties, the strength first increased when the texture index increased and attained a plateau value of approximately 1.4MRD^2. Once again, it was verified that the orientation degree of the mullite was an important factor contributing to the material's mechanical properties. The influence of the shaping process was also illustrated because the sample obtained from casting presented a higher strength. In that case, the leading role of the shaping process can also be assumed in Fig. 4.

Our results showed that the texture index was related to the mullite's orientation degree in the plane of the samples. The orientation degree induced anisotropic elastic and mechanical properties, the former being measured by ultrasonic echography, as in Table 4. Correspondingly, we obtained two specific linear relationships between the anisotropy of the Young's modulus ΔE_{US} and the texture index, shown in Fig. 6. Both relationships were curiously linear and depended on the material composition, further supporting the organization degree in the microstructures, when the addition of muscovite increased the texture index by promoting the preferred orientation of the mullite. This representation of ΔE_{US} according to the texture index showed that not only the shaping method but also many other factors, mainly the processing parameters, were essential to the formation of organized microstructures.

Table 5
Influence of the muscovite addition on the Young's modulus E_0 of the dense material, calculated from the ultrasonic echography and porosity data.

Composition type	Kaolinite	Kaolinite–mica
Porosity (%)	6.8	15.8
E_r (GPa)	116	151
E_z (GPa)	110	138

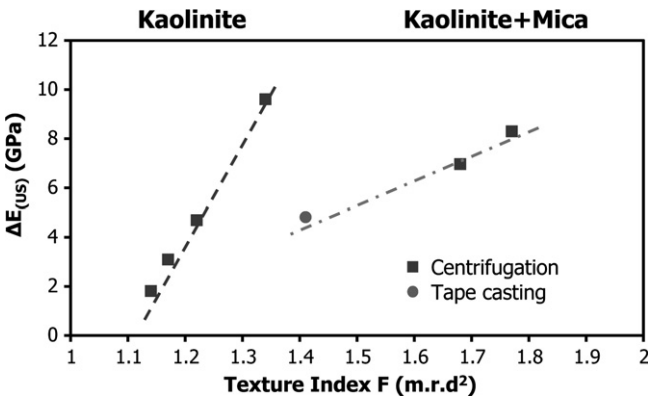

Fig. 6. Correlation between the anisotropy of the Young's modulus ΔE_{US} and the texture index as a function of sample composition.

5. Conclusion

A study of the processing and characterization of micro-composite materials with mullite from kaolinite and muscovite mica revealed the preferential orientations of mullite in sintered materials. Both the Young's modulus and the biaxial flexural strength of the sintered materials were changed by the processing parameters, regardless of the shaping method, such as centrifugation or tape casting. The sintered microstructures were characterized by both the orientation degree obtained with QTA and the open and closed porosities. The Young's modulus and biaxial flexural strength increased with the texture index and attained a plateau value above 1.5MRD^2.

The correlation between the orientation degrees, obtained from the texture index when using QTA, and the anisotropy of the elastic properties showed interestingly linear relationships that were dependent on the material composition.

Acknowledgments

The authors wish to express their gratitude to the European Community (European Social Fund and FEDER) and the Limousin and Basse-Normandie Regions for their financial support of this work.

References

[1] R.E. Mistler, E.R. Twiname, Tape Casting: Theory and Practise, Wiley American Ceramic Society, Westerville, Ohio, 2000.
[2] D. Hotza, P. Greil, Review: aqueous tape casting of ceramic powders, Materials Science and Engineering A202 (1995) 206–217.
[3] Emel Ozel, Semra Kurama, Production of cordierite ceramic by aqueous tape casting process, Journal of Materials Processing Technology 198 (2008) 68–72.
[4] Sen Meia,b, Juan Yangb, Xin Xu, Sandra Quaresma, Simeon Agathopoulos, Josśe M.F. Ferreira, Aqueous tape casting processing of low dielectric constant cordierite-based glass-ceramics—selection of binder, Journal of the European Ceramic Society 26 (2006) 67–71.
[5] S. Deniel, N. Tessier-Doyen, C. Dublanche-Tixier, D. Chateigner, P. Blanchart, Processing and characterization of textured mullite ceramics from phyllosilicates, Journal of the European Ceramic Society 30 (2010) 2427–2434.
[6] S.H. Hong, G.L. Messing, Development of textured mullite by templated grain growth, Journal of the American Ceramic Society 82 (1999) 867–872.
[7] G. Lecomte, P. Blanchart, Textured mullite at muscovite–kaolinite interface, Journal of the European Ceramic Society 41 (2006) 4937–4943.
[8] F. Gridi-Bennadji, D. Chateigner, G. Di Vita, P. Blanchart, Mechanical properties of textured ceramics from muscovite-kaolinite alternate layers, Journal of the European Ceramic Society 29 (2009) 2177–2184.
[9] A. Tucci, L. Esposito, L. Malmusi, E. Rambaldi, New body mixes for porcelain stoneware tiles with improved mechanical characteristics, Journal of the European Ceramic Society 27 (2007) 1875–1881.
[10] O.I. Ece, Z.E. Nakagawa, Bending strength of porcelains, Ceramics International 28 (2002) 131–140.
[11] S.R. Bragança, C.P. Bergmann, A view of whitewares mechanical strength and microstructure, Ceramics International 29 (2003) 801–806.
[12] J.L. Amors, M.J. Orts, J. Garcıa-Ten, A. Gozalbo, E. Sanchez, Effect of the green porous texture on porcelain tile properties, Journal of the European Ceramic Society 27 (2007) 2295–2301.
[13] W.C. Oliver, G.M. Pharr, An improved technique for determining hardness and elastic modulus using load and displacement sensing indentation experiments, Journal of Materials Research 7 (1992) 1564–1583.
[14] W.C. Oliver, G.M. Pharr, Measurement of hardness and elastic modulus by instrumented indentation: advances in understanding and refinements to methodology, Journal of Materials Research 19 (2004) 3–20.
[15] D. Chateigner, D. Ed, Combined analysis: structure-texture-microstructure-phase-stresses-reflectivity analysis by X-ray and neutron scattering (2004). 〈www.ecole.ensicaen.fr/∼chateign/texture/combined.pdf〉.
[16] L. Lutterotti, D. Chateigner, S. Ferrari, J. Ricote, Texture, residual stress and structural analysis of thin films using a combined X-ray analysis, Thin Solid Films 450 (2004) 34–41.
[17] D. Chateigner, Reliability criteria in quantitative texture analysis with experimental and simulated orientation distributions, Journal of Applied Crystallography 38 (2005) 603–611 38.
[18] R.X. Fischer, M. Schmucker, P. Angerer, H. Schneider, Crystal structures of Na and K aluminate mullites, American Mineralogist 86 (2001) 1513–1518.
[19] Crystallography Open Database no. 9005501. Available from: 〈www.crystallography.net〉.
[20] F. Gridi-Bennadji, P. Blanchart, Dehydroxylation kinetic and exfoliation of muscovite flakes, Journal of Thermal Analysis and Calorimetry 90 (2007) 747–753.
[21] J. Schreuer, B. Hildmann, H. Schneider, Elastic properties of mullite single crystals up to 1400 °C, Journal of the American Ceramic Society 89 (2006) 1624–1631.
[22] W. Pabst, E. Gregorova, G. Ticha, Elasticity of porous ceramics: a critical study of modulus–porosity relations, Journal of the European Ceramic Society 26 (2006) 1085–1097.